

average count rate per beam-monitor preset count (BMpc as indicated for the background) at a superlattice reflection resulting from n repetitions. I_0 is the unfolded critical peak intensity, i.e.,

$$I_0 = (\langle I \rangle - B) / \text{IR}(\kappa_1(\Delta T/T)),$$

where IR is the peak intensity reduction due to resolution.¹ A weighted least-squares fit of $I_0 \propto (\Delta T/T)^{-\gamma}$ gave the value of γ , and the number in parenthesis following I_0 is the deviation in % between I_0 and the least-squares fit. The weight w on each point is proportional to the inverse square of the resulting uncertainty on I_0 , i.e.,

$$w = \left\{ \frac{\langle I \rangle I_0^2}{n(\langle I \rangle - B)^2} + I_0^2 \left(1.25 \frac{\delta T}{\Delta T} \right)^2 \right\}^{-1}.$$

Here δT is the uncertainty on ΔT ; we estimated $\delta T \approx 0.1^\circ\text{C}$. It should be noted that if γ is determined from a linear least-squares fit of $\log I_0$ versus $\log(\Delta T/T)$ the weight in this fit is wI_0^2 .

Inverse Correlation Range $a\kappa_1$

κ_1 is the inverse correlation range parameter in the Ornstein-Zernike correlation function $e^{-\kappa_1 r}/r$. a is the cube edge of the unit cell (2.97 Å). $a\kappa_1$ is thus dimensionless. In Type of scan, x means scan along τ_0 and y means scan perpendicular to τ_0 in the scattering plane. A least-squares fit of $a\kappa_1 = k(\Delta T/T_c)^\nu$ gave the values of ν and k , and the number in parenthesis following ($a\kappa_1$) is the deviation in % between $a\kappa_1$ and the least-squares fit. The values of k and ν were used to find $\text{IR}(\kappa_1(\Delta T/T))$ in the evaluation of I_0 .

Long-Range Order and Critical Scattering of Neutrons below the Transition Temperature in β -Brass

J. ALS-NIELSEN AND O. W. DIETRICH

The Danish Atomic Energy Commission, Research Establishment Risø, Roskilde, Denmark

(Received 11 July 1966)

The temperature dependence of long-range order $\langle P_0 \rangle$ has been determined from the temperature variation of a superlattice Bragg reflection. The results fitted a power law $\langle P_0 \rangle \propto (T_c - T)^\beta$ with T_c the critical temperature and $\beta = 0.305 \pm 0.005$, in agreement with the theoretical prediction $0.303 < \beta < 0.318$ obtained from a comparison of the measured line profiles of the (1,0,0) superlattice reflection at 15.5 and 2.2° below T_c . The ratio between the susceptibilities $\chi^+(\Delta T)$ and $\chi^-(\Delta T)$ ΔT deg below and above T_c was found to be 5.5 ± 2.0 at $\Delta T = 4.4^\circ$ and 8.5 ± 3.0 at $\Delta T = 2.1^\circ$. The Ising-model theory predicts the ratio to be 5.2 independent of ΔT .

INTRODUCTION

IN the ordered state in β -brass the Cu and Zn atoms share the sites in the bcc lattice, so Cu atoms predominantly occupy, say, the cube corners and Zn atoms the cube centers of the unit cells. The occupation of lattice site \mathbf{l} is given by the occupation variable $S_{\mathbf{l}}$, which is +1 if site \mathbf{l} is occupied by a Cu atom and -1 if site \mathbf{l} is occupied by a Zn atom.

The long-range order $\langle P_0 \rangle$ is defined as the average of the occupation variable throughout the lattice on the corner sites or the center sites, or the *weighted* average occupation of *all* lattice sites ascribing a weight factor of +1 to the corner sites and -1 to the center sites. The weight factor is conveniently expressed by $e^{i\tau \cdot \mathbf{l}}$, where τ is any vector in reciprocal space with an odd sum of indices (a reciprocal superlattice vector). Thus

$$\langle P_0 \rangle \equiv \frac{1}{N} \sum_{\mathbf{l}} S_{\mathbf{l}} e^{i\tau \cdot \mathbf{l}} \equiv \frac{1}{N} \sum_{\mathbf{l}} P_{\mathbf{l}}. \quad (1)$$

The short-range order is described by the correlation of the occupation of two lattice sites separated by the lattice vector \mathbf{r} . However, to distinguish short-range

order from long-range order, it is only the asymptotically vanishing part $p(\mathbf{r})$ of the pair-correlation function that describes the short-range order, i.e.,

$$p(\mathbf{r}) \equiv \langle P_0 P_{\mathbf{r}} \rangle - \langle P_0 \rangle^2, \quad (2)$$

where

$$\langle P_0 P_{\mathbf{r}} \rangle \equiv \frac{1}{N} \sum_{\mathbf{l}} P_{\mathbf{l}} P_{\mathbf{l}+\mathbf{r}}. \quad (3)$$

Note that $p(\mathbf{r})$ is zero both in the completely ordered state and in the completely disordered state.

When the temperature increases, the long-range order gradually decreases and finally vanishes at the critical temperature T_c . However, the correlation range tends to infinity when T approaches T_c . It is possible to study these phenomena experimentally by means of neutron diffraction. The differential scattering cross section $d\sigma/d\Omega$ at scattering vector $\mathbf{\kappa}$ is given by¹

$$\frac{d\sigma}{d\Omega} \propto N \langle P_0 \rangle^2 \delta(\mathbf{\kappa} - \boldsymbol{\tau}) + \sum_{\mathbf{r}} p(\mathbf{r}) e^{i(\mathbf{\kappa} - \boldsymbol{\tau}) \cdot \mathbf{r}}. \quad (4)$$

¹ J. Als-Nielsen and O. W. Dietrich, second preceding paper, Phys. Rev. **153**, 706 (1966).

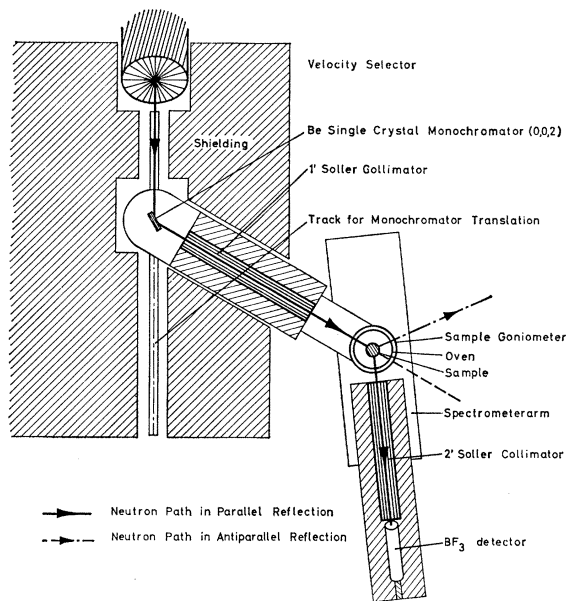


FIG. 1. The diffractometer setup. The neutron paths in the parallel and antiparallel orientations of the sample are shown.

The Ornstein-Zernike pair-correlation function (abbreviated to OZ pcf in the following) proportional to $e^{-\kappa r}/r$ has previously been observed to fit critical-scattering data above T_c .² This pcf implies that the second term in (4) is proportional to $(|\kappa - \tau|^2 + \kappa_1^2)^{-1}$.

An intensity scan through a superlattice reflection below T_c will thus display a narrow Bragg peak superposed on a broad Lorentzian-like peak, the critical scattering. Unfortunately, because of mosaic spread and experimental resolution, the superposition implies that only limited information about $p(\mathbf{r})$ can be obtained below T_c compared to above T_c .

The temperature dependence of $\langle P_o \rangle$ can, however, be determined accurately by the temperature dependence of the Bragg peak intensity. The results were fitted to a power law

$$\langle P_o \rangle \propto (T_c - T)^\beta, \quad T_c - T/T_c \ll 1, \quad (5)$$

and we found $\beta = 0.305 \pm 0.005$.

It is obvious that the ordering of orientations of spins localized on lattice sites can be described in the same way as the ordering of occupation of lattice sites for a binary alloy given above.² In the magnetic case the magnetization M is proportional to $\langle P_o \rangle$ and the susceptibility χ is related to the pair-correlation function by $\chi \propto \sum_{\mathbf{r}} p(\mathbf{r})$.

The power law (5) has been verified experimentally for several magnetic substances and a summary of recent experimental results on the temperature dependence of M can be found in Ref. 3. Most of the experiments indicate that $\beta \approx \frac{1}{3}$.

² M. Fisher, *Lectures in Theoretical Physics* (University of Colorado Press, Boulder, Colorado, 1965), Vol. VII C.

³ M. Eibschütz, S. Shtrikman, and D. Treves, *Solid State Commun.* 4, 141 (1966).

Also a liquid-vapor phase transition is described in terms of occupation variables in the lattice gas model. Here the density difference between the two phases is proportional to $\langle P_o \rangle$.² Among several experiments mention can be made of the measurement of the coexistence curve for Xe by Weinberger and Schneider.⁴ In analyzing their data, Fisher⁵ found $\beta = 0.345 \pm 0.015$.

Most theoretical calculations of β are based on the Ising-model Hamiltonian with nearest-neighbor interaction only. Even with this simplification, an exact solution of the three-dimensional Ising model has not been found yet, and one is compelled to use approximate methods. The classical molecular field theory and cluster theories all give $\beta = \frac{1}{3}$, but more accurate methods have now been developed. Essam and Fisher⁶ obtained

$$0.303 < \beta < 0.318$$

from the Padé approximant procedure used on appropriate low-temperature series. Our result for β is thus in agreement with the Ising model and, in the light of the previously reported results above T_c ,⁷ it is concluded that the order-disorder phenomena in β -brass in the vicinity of T_c are very well described by the Ising model.

MEASUREMENTS AND RESULTS

Apparatus

The diffractometer set up located at the DR-3 reactor is shown in Fig. 1. The monochromatic neutron beam was extracted from the reactor beam by means of Bragg reflection from a Be single crystal with the reflecting (0,0,2) planes parallel to the crystal surface. The wavelength could be changed by translating the monochromator crystal along the reactor beam and thereby changing the angle between the monochromatic

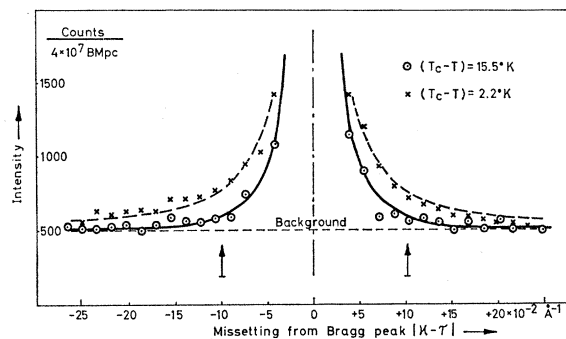


FIG. 2. Intensity scans through (1,0,0) at two temperatures below T_c with $\kappa - \tau$ perpendicular to τ . The tails on the dashed curve are due to critical scattering. The counting time was determined by a monitor in the monochromatic beam preset at 4×10^7 counts (abbr. 4×10^7 BMpc).

⁴ M. A. Weinberger and W. G. Schneider, *Can. J. Chem.* 30, 422 (1952).

⁵ M. Fisher, *J. Math. Phys.* 4, 278 (1963).

⁶ J. W. Essam and M. Fisher, *J. Chem. Phys.* 38, 802 (1963).

⁷ O. W. Dietrich and J. Als-Nielsen, preceding paper, *Phys. Rev.* 153, 711 (1966).

TABLE I. Long-range order data for (1,0,0) reflection. $\lambda = 1.56 \text{ \AA}$.

Thermocouple voltage V (μV)	Average intensity $\langle I \rangle$ from n repetitions		$\sigma(I)$		Background count rate		Count rate from Bragg scattering $I_B^m(V)$	Weight w in LSF (10^{-3})
	$\langle I \rangle$	n	Expt.	Poisson	Constant	Critical scattering		
18 851	7802	8	66	88	192	57	0753	0.89
18 906	6936	21	72	83	192	69	6675	2.88
18 959	6122	25	162	78	192	86	5844	3.92
19 009	5176	31	88	72	192	115	4869	5.81
19 035	4702	6	85	68	192	130	4380	1.06
19 066	4093	3	108	64	192	158	3743	0.50
19 081	3755	5	50	61	192	175	3388	1.06
19 093	3477	11	63	59	192	194	3091	2.88
19 107	3107	28	57	56	192	222	2693	8.70
19 118	2795	7	44	53	192	250	2353	2.15
19 128	2527	14	36	50	192	286	2049	5.13
19 143	2056	28	52	45	192	350	1514	11.50

and the reactor beam. Higher order neutrons were removed by means of a mechanical velocity selector.

The sample crystal was encapsulated tightly in a thin stainless steel container to avoid Zn evaporation, and it was placed in an oven on the goniometer table of the spectrometer. The scattering vector \mathbf{k} could be scanned through the superlattice reflection τ in three perpendicular directions.

Critical Scattering below T_c

The results in this section derive from a 28-mm-diam single crystal of pure β -brass oriented in the (1,0,0) reflection at wavelength 2.70 \AA .

In Fig. 2 are shown two intensity scans through (1,0,0), respectively, at 15.5° and 2.2° below $T_c = 739^\circ\text{K}$. The difference between the two curves is mainly due to critical scattering, but unfortunately this difference is so small that the inverse correlation range κ_1^- ($\Delta T = 2.2^\circ$) cannot be deduced with reasonable accuracy from this measurement.

Using the OZ pcf, I^- becomes

$$I^- = b \frac{1}{|\mathbf{k}-\boldsymbol{\tau}|^2 + (\kappa_1^-)^2} \text{IR}(|\mathbf{k}-\boldsymbol{\tau}|, \kappa_1^-). \quad (6)$$

Here IR is the intensity reduction due to experimental resolution as discussed in detail in Ref. 1. Similarly, the critical intensity I^+ above T_c is given by

$$I^+ = b \frac{1}{|\mathbf{k}-\boldsymbol{\tau}|^2 + (\kappa_1^+)^2} \text{IR}(|\mathbf{k}-\boldsymbol{\tau}|, \kappa_1^+), \quad (7)$$

and b , which depends only slightly on temperature, can therefore be determined from measurement of I^+ since κ_1^+ has been determined previously. Thus, measurement of I^- and I^+ determines κ_1^- . We have measured I^- at a fixed value of $|\mathbf{k}-\boldsymbol{\tau}|$ for $\Delta T = 2.1^\circ$ and $\Delta T = 4.4^\circ$. It is obvious that the most accurate determination of κ_1^- is obtained for the smallest possible value of $|\mathbf{k}-\boldsymbol{\tau}|$. That part of the intensity above the constant background at $|\mathbf{k}-\boldsymbol{\tau}| = 0.10 \text{ \AA}^{-1}$ for $\Delta T = 15.5^\circ$, which might be due to Bragg scattering, will be negligible at $\Delta T = 2.1^\circ$, and at $\Delta T = 4.4^\circ$, and the measurements of I^- were therefore carried out at $|\mathbf{k}-\boldsymbol{\tau}| = 0.10 \text{ \AA}^{-1}$.

The results were $(\kappa_1^-/\kappa_1^+)^2 = 5.5 \pm 2.0$ at $\Delta T = 4.4^\circ$ and $(\kappa_1^-/\kappa_1^+)^2 = 8.5 \pm 3.0$ at $\Delta T = 2.1^\circ$.

Molecular field theory and cluster theories, as well as the more advanced theories of lattice statistics,⁵ predict that the ratio $(\kappa_1^-/\kappa_1^+)^2$ is independent of $T - T_c$ with the values 2 and 5.2, respectively. Although our results are in better agreement with the theories of lattice statistics than with the molecular field theory and cluster theories, the experimental uncertainty is too large for verification of the theories of lattice statistics. An improvement of the experimental accuracy would be desirable and may be obtained with a crystal enriched with Cu⁶⁵; this possibility might be examined in the future.

Temperature Dependence of Long-Range Order

According to (4) the Bragg peak intensity is proportional to the square of the long-range order parameter $\langle P_o \rangle$. The parameter β in (5) can therefore be determined experimentally by measuring the Bragg peak intensity at several temperatures in the vicinity of T_c . In a double log plot of I_B versus $T_c - T$ the results will lie on a straight line with the slope 2β , as shown in Fig. 4.

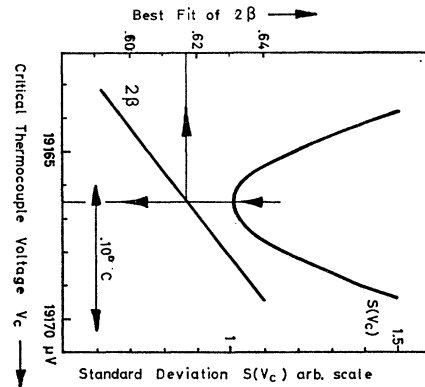


FIG. 3. Least-squares fit of the Bragg peak intensity I_B^m to the power law $I_B = c(V_c - V)^{2\beta}$. For each value of V_c the best values of 2β and c were found and the goodness of the fit given by $S^2(V_c) = \sum_V w(V) (I_B^m(V) - c(V_c - V)^{2\beta})^2$ was calculated. It is concluded that $2\beta = 0.618$ and $V_c = 19166.5 \mu\text{V}$.

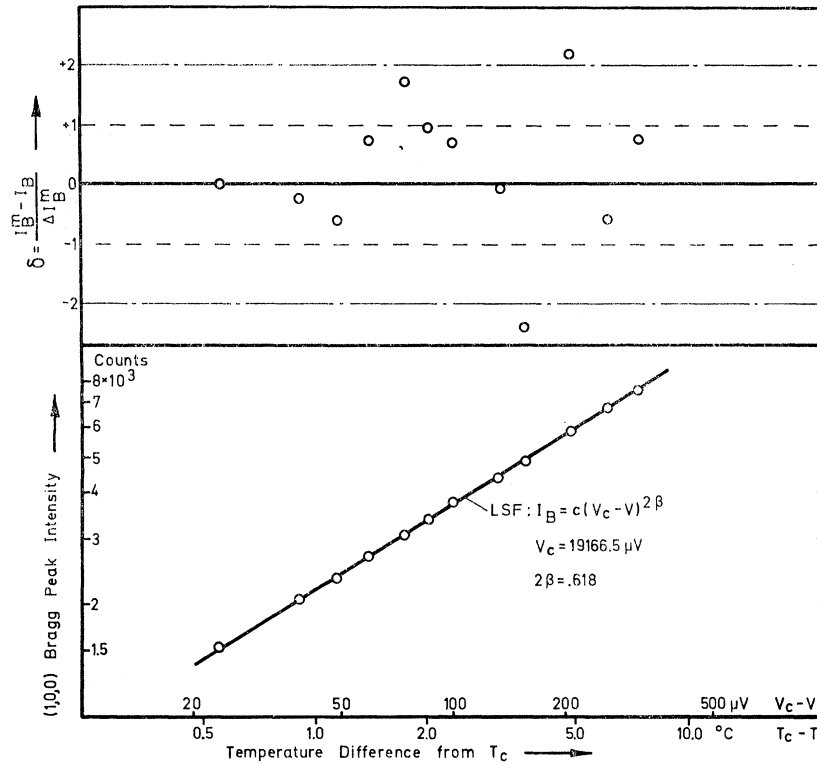


FIG. 4. Double log plot of the Bragg peak intensity versus the temperature difference $T_c - T$ or the thermocouple voltage difference $V_c - V$ with $V_c = 19166.5 \mu\text{V}$. The full line represents a least-squares fit (LSF) to a power law $I_B = c(V_c - V)^{2\beta}$ with $c = 215.2$ and $2\beta = 0.618$. The difference δ between measured and calculated intensities relative to the expected Poisson standard deviation are shown in the upper part of the figure. There is no systematic trend in the deviations and the values of δ indicate that the calculated curve fits the data satisfactorily.

It is, however, presumed that the crystal is similarly irradiated by the neutron beam at all temperatures, i.e., that extinction can be neglected. If present, the extinction will obviously be greater far from T_c than close to T_c , and the measurements will therefore yield a misleadingly small value of β . Furthermore, the low-temperature deviation from the straight line in a double log plot will set in at smaller values of $T_c - T$ in a crystal with extinction than for a crystal without.

The sample used in the critical-scattering measurements was not free from extinction. The temperature dependences of (1,0,0), (1,1,1), and (3,0,0) reflections at 1.35 and at 2.70 Å were not consistent, yielding apparent values of β ranging from approximately 0.20 for the (1,0,0) reflection at 2.70 Å to 0.31 for the (3,0,0) reflection at 1.35 Å, and there was a definite deviation from the straight line in the double log plot only 7° below T_c for the (1,0,0) reflection.

A disk of 2-mm thickness was therefore spark-cut from the 28-mm-diam crystal so as to obtain a sample small enough to be free from extinction. The results given in the remainder of this section derive from this sample.

Measurements from the (1,0,0) reflection in the anti-parallel orientation (see Fig. 1) at 1.56 Å are listed in Table I. At each temperature the peak intensity I_i was measured n times and the average intensity

$$\langle I \rangle = \left(\sum_{i=1}^n I_i \right) / n$$

was calculated. Furthermore, the standard deviation $\sigma(I)$ of a single observation I_i was deduced from the formula

$$\sigma(I) = \left(\sum_{i=1}^n (I_i - \langle I \rangle)^2 / n \right)^{1/2}$$

and compared with $(\langle I \rangle)^{1/2}$, the theoretical standard deviation if the fluctuations on I_i were only due to Poisson statistics. Since reasonable agreement was found for all temperatures, the uncertainty of $\langle I \rangle$ and the associated weight w were calculated from Poisson statistics.

To obtain the Bragg peak intensity I_B^m , a constant background count rate and the peak intensity from critical scattering must be subtracted from $\langle I \rangle$. The latter contribution was deduced as follows:

The critical peak intensity was measured 3° above T_c and the constant b in (7) was determined. Utilizing the experimentally verified 5/4 power law of the unfolded critical peak intensities above T_c , and the theoretical value of the ratio $(\kappa_1^- / \kappa_1^+)^2 = 5.2$ at all temperatures, the peak intensity of critical scattering below T_c was calculated from (6).

The thermocouple voltage V from the cromel-alumel thermocouple depends linearly on the temperature within the range of the measurements, and a weighted least-squares fit (LSF) of $I_B^m(V)$ to the power law

$$I_B = c(V_c - V)^{2\beta}, \quad (8)$$

was carried out for different choices of V_c . The results

for 2β and for

$$S(V_c) = \left\{ \sum_V w(V) (I_B^m(V) - c(V_c - V)^{2\beta})^2 \right\}^{1/2}$$

are shown in Fig. 3. It is concluded that $2\beta = 0.618$ with an estimated uncertainty of ± 0.010 and $V_c = 19\,166.5 \mu\text{V}$. In Fig. 4 is shown I_B^m versus $V_c - V$ in a double log plot, and at the top of Fig. 4 is shown the difference δ between the measured intensities and the least-squares fit relative to the standard deviation of I_B^m . It is concluded that (8) fits the data satisfactorily.

Similar measurements were carried out for (1,0,0) and (1,1,1) reflections in the parallel orientation and results were, respectively, $(2\beta, V_c) = (0.592, 19\,167.6 \mu\text{V})$ and $(2\beta, V_c) = (0.593, 19\,168.6 \mu\text{V})$. In a double log plot like Fig. 4 no deviation from a straight line was apparent down to temperatures 25° below T_c .

The consistency of these three sets of data give confidence to the assertion:

$$\beta = 0.305 \pm 0.005.$$

CONCLUSION

The temperature dependence of long-range order in the vicinity of the critical temperature T_c has been deduced from the temperature dependence of the peak intensity from a superlattice reflection. It is essential for proper interpretation of the data that extinction is negligible; in the present work this was obtained by

using a small sample (2-mm thickness) at medium wavelength (1.56 Å). Consistent results were found from the (1,1,1) and (1,0,0) reflections in the parallel and the antiparallel orientations. Background count rate due to critical scattering was subtracted and the resulting intensity I_B obeyed the power law $I_B \propto (T_c - T)^{2\beta}$ with $\beta = 0.305 \pm 0.005$, in agreement with the prediction of the Ising model. Values of β found in magnetic systems are generally slightly greater than the value we observed for the alloy, and this might indicate a small difference between a Heisenberg and an Ising magnet as regards the temperature dependence of long-range order.

The neutron-diffraction method can in principle also be used to determine the temperature dependence of the susceptibility and the correlation range of short-range order below T_c . Unfortunately the accuracy suffers seriously by the superposition of a Bragg peak on the critical scattering. We have determined the square of the ratio between the inverse correlation ranges ΔT below and above T_c and found $(\kappa_1^-/\kappa_1^+)^2 = 8.5 \pm 3.0$ at $\Delta T = 2.1^\circ$ and $(\kappa_1^-/\kappa_1^+)^2 = 5.5 \pm 2.0$ at $\Delta T = 4.4^\circ$. The prediction of the Ising model is $(\kappa_1^-/\kappa_1^+)^2 = 5.2$ independent of mT . Improvement of the accuracy for critical scattering below T_c would be of considerable interest and may be obtained with a crystal enriched with Cu⁶⁵.

Fermi Surface of Pb under Hydrostatic Pressure*

J. R. ANDERSON

University of Maryland, College Park, Maryland

AND

W. J. O'SULLIVAN AND J. E. SCHIRBER

Sandia Laboratory, Albuquerque, New Mexico

(Received 17 June 1966; revised manuscript received 1 August 1966)

Measurements of the effect of hydrostatic pressure on the Fermi surface of lead are reported. The frequencies of the α , β , and γ oscillations were all found to increase by about 0.3% kbar^{-1} , a rate more than twice that expected from scaling of the Fermi surface with volume. The pressure results on the β oscillations provide evidence for the association of these oscillations with the ν orbit. Estimates of the variations with pressure of the Fourier coefficients of the pseudopotential are obtained, as well as estimates of the average values of the diagonal components of Pippard's deformation parameter for the three orbits. Our results suggest that simple pseudopotential-model calculations can give at best a qualitative estimate of the potential change resulting from small variations of the wave vectors with pressure.

INTRODUCTION

THE de Haas-van Alphen (dHvA) effect has been used by Anderson and Gold¹ to determine the Fermi surface of lead. Although a reasonable description was obtained, there was some uncertainty in the assign-

ment to a particular section of the Fermi surface of the very strong β oscillations. These oscillations were attributed to an electron orbit ν in the third band formed by the intersection of four {110} "arms" (Fig. 1), which was by far the most reasonable choice, but a second possibility was to assign the oscillations to a third-band hole orbit ξ lying in the square face of the Brillouin zone. Pressure studies provide additional evi-

* Supported in part by the U. S. Atomic Energy Commission and by the Advanced Research Projects Agency.

¹ J. R. Anderson and A. V. Gold, Phys. Rev. **139**, 1459 (1965).